Front. Electr. Electron. Eng. China 2008, 3(1): 123–128
DOI 10.1007/s11460-008-0011-9

RESEARCH ARTICLE

Laisheng TONG, Guangning WU, Tongguang LIN, Guoqin ZHANG, Xi LIU

Study on voltage distribution in windings of an inverter-fed traction motor

Abstract Voltage distribution in windings is important for inverter-fed traction motors. The analysis on voltage distribution characteristics is significant to the study of insulation failure mechanisms and structure design. First, a distribution parameter model has been developed according to the winding structure of an inverter-fed traction motor. Based on the model, finite element differential method was employed to determine voltage distribution characteristics. Simulation results were compared with actual voltage distribution. Moreover, the influence of pulse rise time and cable was discussed. The results show that the shorter the pulse rise time is, the more uneven the voltage distribution is. In addition, cable length has little influence on voltage distribution characteristics. However, the amplitude of voltage would also increase by 40% in coils and turns.

Keywords traction motor, winding, voltage distribution, pulse, cable

1 Introduction

With the progress of fast power switching devices such as the insulated gate bipolar transistor (IGBT), pulse width modulation (PWM) inverter-fed traction motors have become widely used in express locomotives [1,2]. To decrease harmonic content in the current and voltage of inverter-fed traction motors, switching frequency and dv/dt of the inverter are very high (20 kHz, 2500 V/μs). Repetitive steep-fronted pulses not only cause over-voltage on the terminal of a traction motor, but also result in an uneven voltage distribution in the windings. Partial discharges brought by over-voltage in traction motors would result in premature failure of insulation [3,4]. Measurement results obtained by A. Mbaye, Pierre Bidan and D. B. Hyypio show that the highest stress is located across the first few turns of the first coil [5–7]. The same results were achieved by L. Gubbala and G. Suresh utilizing equivalent circuits [8,9]. The transmission line theory is used to analyze voltage distribution in motor windings by J. L. Guardao and C. Petrarca [10,11] and the results indicate that voltage distribution relates to the rise time of pulse and the construction parameter of windings, and the highest turn-to-turn stress is located across the last turn of the first coil. A. Narang [12] thinks that 70–120% of the pulse voltage is located across the first coil, but the highest turn-to-turn stress is not on the last turn for all inverter-fed motors – it depends on the turn number of windings and motor construction.

Voltage distribution characteristics of windings of inverter-fed motor are currently not definitive. The traditional design criterion of AC motors is not suitable for inverter-fed motor design. The effective criterion must be adopted to face voltage distribution uniformity and other problems. Consequently, research on voltage distribution characteristics of inverter-fed traction motors is very important to improve the quality of traction motors.

In the present paper, a distribution parameter model has been developed according to the winding structure of an inverter-fed traction motor. Based on the model, finite element differential method is used to get the voltage distribution characteristics. Moreover, some available experimental data of real traction motors are compared with numerical results. Then with this model, the influence of pulse rise-time and cable length on voltage distribution characteristics is studied.

Translated from *Proceedings of the Chinese Society for Electrical Engineering*, 2006, 26(12): 134–138 [译自: 中国电机工程学报]

Laisheng TONG (✉)
Zhuzhou Electrical Locomotive Co. Ltd., Zhuzhou 412001, China
E-mail: alanatlsh@126.com

Guangning WU, Tongguang LIN, Guoqin ZHANG, Xi LIU
School of Electrical Engineering, Southwest Jiaotong University, Chengdu 610031, China

2 Traction motor winding model

Fourier analysis of the PWM pulse defines an equivalent upper limit frequency f_u that corresponds to pulse rise-time. f_u for various pulse rise-time can be calculated by Eq. (1) [13]:

$$f_u = \frac{1}{\pi t_{rise}}, \tag{1}$$

where t_{rise} is pulse rise-time, f_u is equivalent upper limit frequency and f_u is up to MHz.

An accurate high-frequency equivalent circuit model of the winding components is essential to simulate transient voltage distribution. The stator of a traction motor has a two-layer winding, and two adjacent coils are located in different slots. The eddy current near the surface of the adjacent turns and the iron slot walls shield away most of the flux. As a result, electromagnetic coupling of coils in different slots can be neglected. Mutual inductance exists only between the immediately adjacent turns. In one coil, only turn-to-turn capacitance and turn-to-ground capacitance are considered. After the model for a coil of the traction motor stator has been analyzed, the equivalent circuit of the winding shown in Fig. 1 can be obtained by cascading the individual turn models. Each turn is described by concentrated parameters such as resistance R, self-inductance L, turn-to-turn mutual inductance M, turn-to-turn capacitance C_t and turn-to-ground capacitance C_g. C_{t1} and C_{t4} are half of C_t. C_{g0} and C_{g4} are half of first turn-to-ground capacitance C_g.

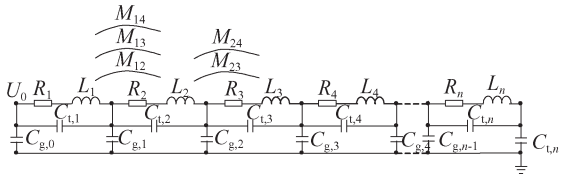

Fig. 1 Equivalent circuit of winding for simulation

Lamination iron core can be considered as a whole body when coil capacitance is calculated [14]. Consequently, turn-to-turn capacitance and turn-to-ground capacitance can be calculated by using the parallel-plate capacitor formula, which can be calculated from Eqs. (2), (3) and (4). Dielectric constant of compound insulation material is computed by Eq. (5).

$$C_t = \frac{\varepsilon_t w l}{d_t}, \tag{2}$$

$$C_{g(2,3)} = \frac{4\varepsilon_g h l_g}{d_g}, \tag{3}$$

$$C_{g(1,4)} = \frac{4\varepsilon_g h l_g + \varepsilon_g w l_g}{d_g}, \tag{4}$$

$$\frac{d}{\varepsilon_g} = \sum_{i=1}^{n} \frac{d_i}{\varepsilon_i}. \tag{5}$$

Here, ε_t and ε_g are the relative permittivity of turn-to-turn and turn-to-ground compound insulation materials respectively, while ε_i is the relative permittivity of each kind of insulation material. d_i is the thickness of each kind of insulation material, d_t is the thickness of turn insulation, and d_g is the thickness of ground insulation. w is the conductor width, h is the conductor height, l is the length of one turn, and l_g is the length of slot.

Due to longitudinal losses brought by the skin effect, the propagation wave is not transverse electromagnetic. However, the serial resistance remains a small factor to longitudinal impedance. Therefore, the assumption of transverse electromagnetics is adequate when the duality principle between the electric and magnetic fields is adopted to derive the total capacitance of a unit length of a turn. The inductance matrix $\boldsymbol{L}$ has been calculated by means of the relationship $LC_0 = \varepsilon_0\mu_0\boldsymbol{I}$, where ε_0 and μ_0 are the permittivity and permeability of free space respectively, $\boldsymbol{I}$ is the identity matrix, and C_0 is the capacitance in free space. In view of the skin effect, copper losses R can be calculated by Eq. (6), where l is the length of a turn, A is the area, and δ is the skin depth given by Eq. (7), in which f is the frequency and σ is copper conductivity.

$$R = \frac{l}{A\delta\sigma}, \tag{6}$$

$$\delta = \frac{1}{\sqrt{\pi f \mu_0 \mu_r \sigma}}. \tag{7}$$

3 Solution by detailed model and finite-difference method

U_0 is the input voltage in the equivalent circuit as shown in Fig. 1. We can obtain Eq. (8) by applying Kirchhoff's current law,

$$i_j - i_{j+1} = C_{g,j}\frac{\mathrm{d}(U_0 - \sum_{m=1}^{j} u_m)}{\mathrm{d}t} - C_{t,j}\frac{\mathrm{d}u_j}{\mathrm{d}t} + C_{t,j+1}\frac{\mathrm{d}u_{j+1}}{\mathrm{d}t}. \tag{8}$$

According to Eq. (8), a differential equation $\boldsymbol{Y}(\mathrm{d}\boldsymbol{U}/\mathrm{d}t) = \boldsymbol{I}$ can be derived. Using single time-step Δt differentiation, it becomes $\boldsymbol{Y}\boldsymbol{U}^{(k+1)} = \Delta t\boldsymbol{I}^k + \boldsymbol{Y}\boldsymbol{U}^k$, where

$$\boldsymbol{Y}=\begin{bmatrix} \sum_{m=1}^{n} C_{g,m} & -\sum_{m=1}^{n} C_{g,m}-C_{t,1} & -\sum_{m=2}^{n} C_{g,m} & \cdots & -\sum_{m=n-1}^{n} C_{g,m} & -C_{g,n} \\ \sum_{m=2}^{n} C_{g,m} & -\sum_{m=2}^{n} C_{g,m} & -\sum_{m=2}^{n} C_{g,m}-C_{t,2} & \cdots & -\sum_{m=n-1}^{n} C_{g,m} & -C_{g,n} \\ \vdots & \vdots & & & \vdots & \\ \sum_{m=n-1}^{n} C_{g,m} & -\sum_{m=n-1}^{n} C_{g,m} & -\sum_{m=n-1}^{n} C_{g,m} & \cdots & -\sum_{m=n-1}^{n} C_{g,m}-C_{t,n-1} & -C_{g,n} \\ C_{g,n} & -C_{g,n} & -C_{g,n} & \cdots & -C_{g,n} & -C_{g,n}-C_{t,n} \end{bmatrix} \tag{9}$$

From Fig. 1, via Kirchhoff's voltage law, we can obtain

$$u_j = L_j\frac{\mathrm{d}i_j}{\mathrm{d}t} + M_{j-1,j}\frac{\mathrm{d}i_{j-1}}{\mathrm{d}t} + M_{j,j+1}\frac{\mathrm{d}i_{j+1}}{\mathrm{d}t} + M_{j,j+2}\frac{\mathrm{d}i_{j+2}}{\mathrm{d}t} + R_j i_j. \tag{10}$$

According to Eq. (10), through single time-step Δt differentiation, the differential equation $\mathbf{Z}(\mathrm{d}\boldsymbol{I}/\mathrm{d}t)=\boldsymbol{U}_Z$ turns into $\boldsymbol{ZI}^{(k+1)}=\Delta t\boldsymbol{U}_Z^k+\boldsymbol{ZI}^k$, where

$$\boldsymbol{Z}=\begin{bmatrix} L_1 & M_{1,2} & M_{1,3} & M_{1,4} & & \\ M_{1,2} & L_2 & M_{2,3} & M_{2,4} & & \\ & & \vdots & \vdots & \vdots & \\ & & M_{n-3,n-1} & M_{n-2,n-1} & L_{n-1} & M_{n-1,n} \\ & & M_{n-3,n} & M_{n-2,n} & M_{n-1,n} & L_n \end{bmatrix}. \tag{11}$$

Here, $\boldsymbol{U}_Z=[u_1-R_1i_1,\ldots,\ u_j-R_ji_j,\ \ldots,\ u_n-R_ni_n]$, $\boldsymbol{I}=[i_1,\ \ldots,i_j,\ldots,\ i_n]$, u_j is the voltage across jth turn, i_j is the electrical current of jth turn, and $j=1,\ 2,\ \ldots,\ n$, n is the number of turns. Then, Eq. (12) is derived from Eqs. (10) and (11) and voltage distribution in windings is given by solving Eq. (12):

$$\begin{cases} \boldsymbol{YU}^{(k+1)}=\Delta t\boldsymbol{I}^k+\boldsymbol{YU}^k \\ \boldsymbol{ZI}^{(k+1)}=\Delta t\boldsymbol{U}_Z^k+\boldsymbol{ZI}^k \end{cases}. \tag{12}$$

The surge voltage here is characterized by the rise time 50 ns and the value is 1 kV. It has been applied into the windings. Voltage distribution and wave-shapes of the first five coils is shown in Fig. 2. The maximum voltage is located on the first coil, and the value is up to 80% of the surge voltage. Voltages of other coils decrease in turn. In view of the maximum voltage on the first coil, inter-turn voltage distribution of the first coil is analyzed in detail. As shown in Fig. 3, the highest surge voltage is located on the first turn. Also, the secondary high voltage is across the second turn. The highest surge voltage is approximately 1.5 times the minimum voltage.

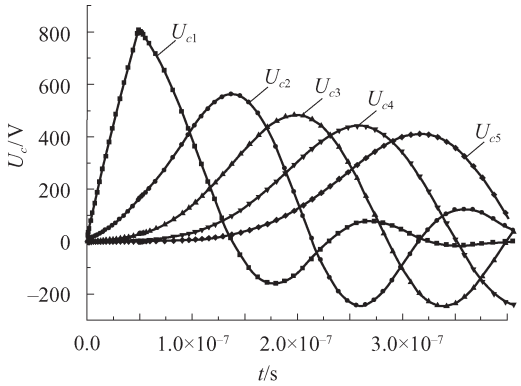

Fig. 2 Voltage distribution of coils

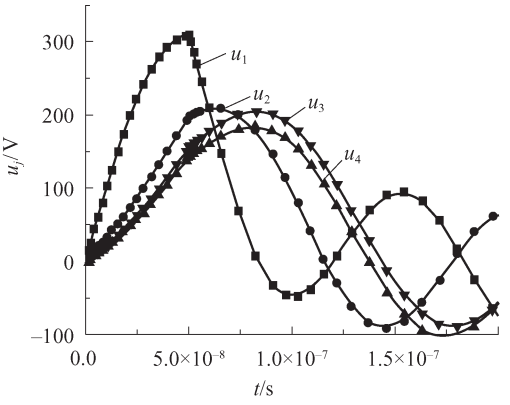

Fig. 3 Voltage distribution of turns of the first coil

The single pulse produced by the high frequency pulse generator (IRCO) is considered as surge voltage to measure voltage distribution in windings. The rise-time of single pulse is 50 ns and voltage magnitude is 100 V. Measurement results can be compared with the corresponding simulation results as shown in Fig. 4. The analysis shows a good correlation between the measured and computed results. It is verified that an equivalent circuit of windings can be applied to accurate analysis of voltage distribution in traction motor windings.

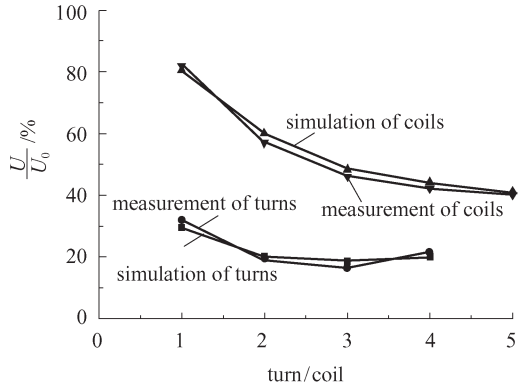

Fig. 4 Comparison of measured and simulated results

4 Influence of rise-time of pulse

It is known that the rise-time of pulses produced by inverters depends on conduction time of power semiconductors such as a gate turnoff thyristor (GTO) (typically 1 μs,), giant transistor (GTR) (typically, 0.5 μs), and insulated gate bipolar transistor (IGBT) (typically, 0.1 μs). The simulations have been carried out using the equivalent circuit. It has been found that the maximum voltage sensibly varies with the rise time in Figs. 5 and 6. For each coil and turn, it maximum voltage is reached with the shorter rise-time. The inter-turn voltage is uniformly distributed in the slot when the rise-time is longer than 1 μs. Inter-turn voltages have the same varying tendency with coil voltages. There is no change of coil voltage distribution characteristic when the rise-time varies. But the characteristic of inter-turn voltage distribution is changed by different maximum voltage locations. Different structures of random and form windings give rise to many differences in voltage distribution in the papers [5–9] and the papers [10–12] respectively. The form windings discussed in this paper are different from those in Refs. [10–12]. Therefore, the result is not in accord. These aspects indicate that the winding structure can be one of the factors influencing voltage distribution in windings.

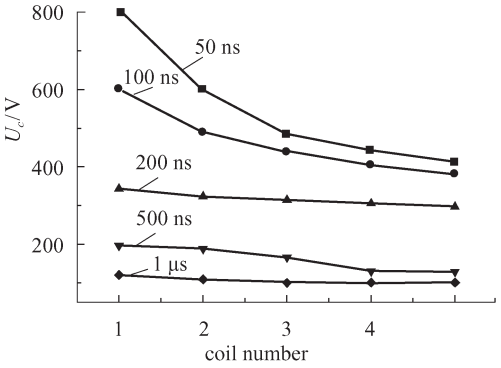

Fig. 6 Voltage distribution of coils with different rise-times

5 Influence of cable

Inverters and motors are installed at different locations in the traction speed regulating system of express locomotives and thus require long connecting cables. Relying on the surge impedances of the cable and traction motor, the traction motor terminal voltage can be much higher than the DC bus value. In terms of two-port network representation and transmission line theory, transmission process of the wave in the cable can be written as:

$$\begin{bmatrix} U_{\mathrm{I}} \\ I_{\mathrm{I}} \end{bmatrix} = \begin{bmatrix} \mathrm{ch}\gamma x & -Z_{\mathrm{c}}\mathrm{sh}\gamma x \\ -\mathrm{sh}\gamma x/Z_{\mathrm{c}} & \mathrm{ch}\gamma x \end{bmatrix} \begin{bmatrix} U_0 \\ I_0 \end{bmatrix} \tag{13}$$

where $\mathrm{ch}\gamma x = (\mathrm{e}^{\gamma x} + \mathrm{e}^{-\gamma x})/2$, $\mathrm{sh}\gamma x = (\mathrm{e}^{\gamma x} - \mathrm{e}^{-\gamma x})/2$, $\gamma = \sqrt{(R_{\mathrm{c}} + \mathrm{j}\omega L_{\mathrm{c}})(G_{\mathrm{c}} + \mathrm{j}\omega C_{\mathrm{c}})}$, $Z_{\mathrm{c}} = \sqrt{(R_{\mathrm{c}} + \mathrm{j}\omega L_{\mathrm{c}})/(G_{\mathrm{c}} + \mathrm{j}\omega C_{\mathrm{c}})}$, R_{c}, L_{c}, G_{c}, C_{c} are the resistance, inductance, conductance, capacitance of the cable in unit length respectively, x is the cable length, and U_{I} and I_{I} are the voltage and current of traction inverter output. As shown in Fig. 7, the longer cable leads to higher over-voltage in the

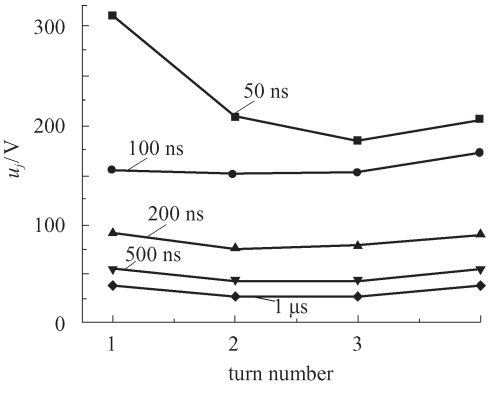

Fig. 5 Voltage distribution of turn to turn of first coil with different rise-times

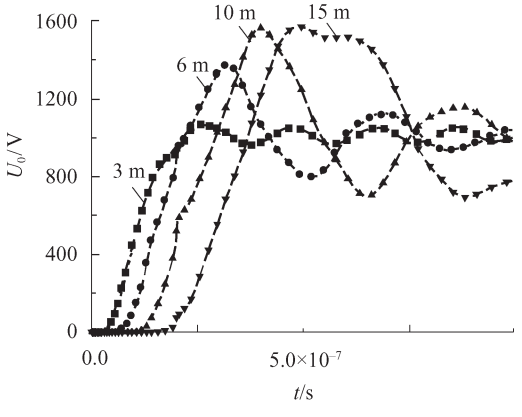

Fig. 7 Over-voltage of traction motor terminal with different lengths of cable

traction motor terminal. But when the length of the cable is longer than 10 m, over-voltage value does not increase any more. The same aspects have been met in Refs. [15–17]. It is possible to identify a critical value for the cable length, for which the over-voltage is at maximum. Here, the rise-time of surge voltage is twice the time of wave transmission in the cable. Over-voltage value can be calculated by $(1+\beta)U_{\mathrm{I}}$, where β is the reflection coefficient of traction motor terminal. Voltage distributions of traction motor windings with different lengths of cable are shown in Figs. 8 and 9. Voltage distribution characteristics will not change with the length of cable, but voltage values increase by 40%. It is found that the inter-turn voltage is almost independent of the length of the connecting cable. But the length of the cable has a strong influence on inter-coil voltage.

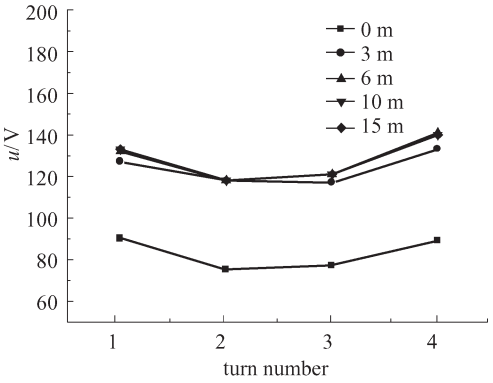

Fig. 8 Voltage distribution of turn to turn of first coil with different lengths of cable

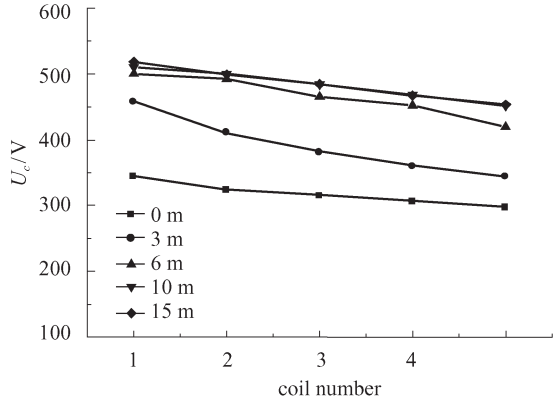

Fig. 9 Voltage distribution of coils with different lengths of cable

6 Conclusions

This paper has presented an analysis of voltage distribution in molded windings of an inverter-fed traction motor. Due to the feeder cable between the traction inverter and motor, the system has been studied by means of a distribution parameter model.

1) The location of the maximum inter-turn voltage varies with the rise-time of pulse. As a whole, the voltage amplitudes of the first and the last turn are larger. Voltage distribution characteristics in windings do not vary with the rise-time of pulse. But the voltage values of coils will change. The voltage distribution in windings remains uniform if the rise-time is longer than 1 μs.

2) Due to the unmatched surge impedances of the cable and traction motor, the over-voltage occurs at the traction motor terminal. Longer cables lead to higher over-voltage. When the cable length is longer than 10 m, over-voltage value reaches its maximum with no further increase. Simulation results show a sensitive dependence of voltage distribution in windings on the rise-time of pulse and winding structure. Voltage distribution characteristics will not change with the cable length, but voltage values would increase by 40%.

Acknowledgements This work was supported by the National Natural Science Foundation of China (Grant No. 50377035) and Fok YindTung Education Foundation (No. 91060).

References

1. Tan X Y. Advanced SHEPWM technique for ac traction drives. Proceedings of the CSEE, 2001, 21(9): 47–52 (in Chinese)
2. Zou Z B, Cai L J, Gan H X. Nonlinear decoupling control of three phase voltage source SPWM inverter. Proceedings of the CSEE, 2004, 24(10): 57–60 (in Chinese)
3. Wheeler J C G. Effects of converter pulses on the electrical insulation in low and medium voltage motors. IEEE Electrical Insulation Magazine, 2005, 21(2): 22–29
4. Fabiani D, Montanari G C, Cavallini A, et al. Relation between space charge accumulation and partial discharge activity in enameled wires under PWM-like voltage waveforms. IEEE Transactions on Dielectrics and Electrical Insulation, 2004, 11(3): 393–405
5. Mabye A, Bellomo J P, Lebey T, et al. Electrical stresses applied to stator insulation in low-voltage induction motors fed by PWM drives. IEE Proceedings Electric Power Applications, 1997, 144(3): 191–198
6. Bidan P, lebey T, Montseny G, et al. Transient voltage distribution in inverter fed motor windings experimental study and modeling. IEEE Transactions on Power Electronics, 2001, 16(1): 92–100
7. Hyypio D B. Simulation of cable and winding response to steep fronted voltage waves. In:Proceedings of the 1995 Industry Applications Society Conference, Orlando: FL. 1995, 1: 800–806
8. Gubbala L, von Jouanne A, Enjeti P, et al. Voltage distribution in the windings of an Ac motor subjected to high dv/dt PWM voltages. 26th Annual IEEE Power Electronics Specialists Conference, USA : Atlanta. 1995, 1: 579–585
9. Suresh G, Toliyat H A, Rendusara D A, et al. Predicting the transient effects of PWM voltage waveform on the stator windings of random wound induction motors. IEEE Transactions on Power Electronics, 1999, 14(1): 23–30
10. Guardado J L, Carrillo V, Cornick K J. Calculation of interturn voltages in machine windings during switching

transients measured on terminals. IEEE Transactions on Energy Conversion, 1995, 10(1): 87–94
11. Petrarca C, Maffucci A, Tucci V, et al. Analysis of the voltage distribution in a motor stator winding subjected to steep-fronted surge voltages by means of a multiconductor lossy transmission line model. IEEE transactions on Energy Conversion, 2004, 19(1): 7–17
12. Narang A, Gupta B K, Dick E P, et al. Measurement and analysis of surge distribution in motor stator windings. IEEE transactions on Energy Conversion, 1989, 4(1): 126–134
13. Skibinski G, Kerkman R, Leggate D. Reflected wave modeling techniques for PWM AC motor drives. Applied Power Electronics Conference and Exposition, USA: Anaheim. 1998, 2: 1021–1029
14. Xian Z L, Jiang J G, Cao H X. The effect of structure and frequency characteristic of dielectric constant on capacitance of electrical machine stator winding. Proceedings of the CSEE, 2004, 24(8): 129–133 (in Chinese)
15. Ma H F, Xu D G, Chen X Y, et al. Research of voltage reflection of PWM inverter-fed induction motor with long motor leads. Proceedings of the CSEE, 2001, 21(11): 109–113 (in Chinese)
16. Liu X Z, Xu C X. Suppression of overvoltage acting on the terminal of PWM inverter-fed motor. Proceedings of the CSEE, 2001, 21(8): 84–88 (in Chinese)
17. Wan J R, Lin Z Q, Yu H J. Research on motor terminal over-voltage caused by high-frequency PWM pulse. Proceedings of the CSEE, 2001, 21(11): 43–47 (in Chinese)